Degradation of MAC13243 and studies of the interaction of resulting thiourea compounds with the lipoprotein targeting chaperone LolA.

Courtney Barker [a], Sarah Allison [a], Soumaya Zlitni [a], Nick Duc Nguyen [b], Rahul Das [b], Giuseppe Melacini [b], Alfredo A Capretta [b] and Eric D Brown [a]

[a] Department of Biochemistry and Biomedical Sciences, McMaster University, 1280 Main Street West, Hamilton, ON L8S 2K1

[b] Department of Chemistry and Chemical Biology, McMaster University, 1280 Main Street West, Hamilton, ON L8S 4M1

Corresponding author. Tel +1 905 525-9140 x22454; fax: +1 905 522 9033. Email address: ebrown@mcmaster.ca (E. Brown)

Abstract

The discovery of novel small molecules that function as antibacterial agents or cellular probes of biology is hindered by our limited understanding of bacterial physiology and our ability to assign mechanism of action. We previously employed a chemical genomic strategy to identify a novel small molecule, MAC13243, as a likely inhibitor of the bacterial lipoprotein targeting chaperone, LolA. Here, we report on the degradation of MAC13243 into the active species, *S*-(4-chlorobenzyl)isothiourea. Analogs of this compound (for example, A22) have previously been characterized as inhibitors of the bacterial actin-like protein, MreB. Herein, we demonstrate that the antibacterial activity of MAC13243 and the thiourea compounds are similar; these activities are suppressed or sensitized in response to increases or decreases of LolA copy number, respectively. We provide STD NMR data which confirms a physical interaction between LolA and the thiourea degradation product of MAC13243, with a K_d of ~150 μM. Taken together, we conclude that the thiourea series of compounds share a similar cellular mechanism that includes interaction with LolA in addition to the well-characterized target MreB.

Keywords

Chemical Biology; structure-activity relationship; lipoprotein trafficking; LolA; MreB; chemical-genetic interactions

Small molecules have a proven track record not only as antibiotics but also as probes of bacterial physiology [1]. Thus the discovery of new antibacterial molecules is a promising approach to the creation of new tools to understand bacterial systems. While connecting cellular phenotype of a small molecule and its molecular target(s) remains a significant challenge, chemical genomic approaches are finding broad application in defining mechanisms of action of new chemical probes [2]. Our group previously employed such a chemical genomic strategy to identify cellular targets of novel small molecules discovered in screens for growth inhibition of the model microbe *E. coli*. Of interest, the inhibitory action of a novel compound, MAC13243, was suppressed when the lipoprotein chaperone, *lolA*, was expressed at high copy [2c]. LolA, part of the five-membered Lol (localization of lipoproteins) system, is responsible for the sorting and transport of lipoproteins to the outer membrane in the majority of Gram-negative bacteria [3]. Further biochemical and physiological experiments confirmed that MAC13243 interacted with LolA to inhibit the localization of lipoproteins to the outer membrane.

Since the original identification of MAC13243 as a probe of lipoprotein targeting, we have discovered that it is unstable in aqueous solution and its triazine ring is slowly hydrolyzed. Herein, we report on the breakdown of MAC13243 (compound **1** in this work) to 3,4-dimethoxyphenethylamine (**2**) and *S-(*4-chlorobenzyl)isothiourea (**3a**) (Figure 1). The latter we suggest is the chemical entity responsible for the antibacterial activity associated with **1**. Compound **3a** is a structural analog of A22 (*S*-(3,4-dichlorobenzyl)isothiourea), a small molecule previously reported to inhibit the bacterial actin-like protein MreB. A22 was originally identified in a screen for inhibitors of chromosome partitioning based upon its ability to induce a morphological change from rod-shaped to spherical [4]. Mutations conferring resistance to A22 isolated in both *Caulobacter crescentus* and *Escherichia coli* mapped to the ATP-binding pocket of MreB [5]. Further biochemical characterization suggested that A22 competitively inhibits the binding of ATP to MreB, leading to the disassembly of actin filaments [6]. With the discovery that **1** could break down to an active species that was a close analogue of A22, we have further

explored the chemical-genetic interactions of *lolA* with A22 and related thiourea-containing compounds.

In order to investigate the *in vitro* stability of **1**, samples (250 µM) were incubated under acidic, neutral or basic conditions for up to 48 hours at room temperature and analyzed using reverse phase HPLC. At time zero, compound **1** elutes as a single peak at the 8 minute mark (Figure 2A, DMSO). However, after incubation in weakly acidic aqueous solution, the appearance of two additional peaks is observed (Figure 2A, pH 4). Quantification of these peaks over time revealed that **1** is indeed unstable in aqueous solution and that its half-life is pH dependent (Figure 2B). Under acidic conditions **1** was shown to have a half-life of ~4 hours, whereas under neutral or basic conditions the compound has a half-life of 13 and 59 hours, respectively. The stability of compound **1** in the organic solvent DMSO, used routinely to dissolve and store frozen working stocks of the compound, was also tested. In this solvent, **1** was found to be relatively stable, with a half-life of 257 hours at room temperature. These findings support (acid-catalyzed) hydrolysis of the central triazine ring of compound **1**. As such, hydrolysis of one molecule of **1** would generate one molecule of 3,4-dimethoxyphenethylamine (**2**), one molecule of *S-(*4-chlorobenzyl)isothiourea (**3a**), and two molecules of formaldehyde.

Subsequent analysis of the biological activity of each degradation product revealed that, of the breakdown products **2** and **3a**, the latter compound was the active species (Figure 3). Based on these results, we hypothesized that degradation into the compound **3a** could be responsible for the biological activity associated with compound **1**. Previous structure activity relationship (SAR) data for **1** supported this hypothesis, as major structural changes on the left-hand side of the molecule, corresponding to the inactive degradation product **2**, did not significantly affect biological activity[2c]. The same was not true for the right-hand side of the molecule, where major structural modifications were not tolerated. Furthermore, **3a** was found to be four-fold more potent than MAC13243 (Figure 3). The interpretation of this finding was compounded by the realization that **3a** is a structural analog of *S*-(3,4-

dichlorobenzyl)isothiourea, known as A22 in the literature, which has been reported to inhibit the bacterial cytoskeleton protein, MreB [5-6]. To shed light on this paradox, we set out to explore the existence of a possible chemical genetic interaction between the thiourea series of compounds and *lolA*.

We originally identified a chemical genetic interaction between the lipoprotein chaperone, LolA, and compound **1** using an ordered high-copy expression array [2c]. The growth inhibitory action of the small molecule was suppressed by the presence of the protein target at high copy. Using an inducible expression system, we examined whether LolA at high copy could also suppress the inhibitory actions of compound **3a** and A22. Cultures overexpressing *lolA* (pCA24N-*lolA*) or containing empty expression vector (pCA24N) were spotted on LB agar plates containing increasing concentrations of **1**, **3a** or A22. Overexpression of *lolA* increased the MIC 16-fold for each of the three compounds (Figure 4). The ability of LolA at high-copy to suppress the action of compound **3a** and A22 suggests that these breakdown products share a similar cellular mechanism to the parent compound, **1**. Further, these data provide the first evidence of a chemical genetic link between A22 and *lolA*.

Next we examined the effect of reduction of LolA copy number in cells. Reducing expression of a cellular target typically enhances the growth inhibition phenotype caused by a small molecule [2d, 7]. Using a conditional *lolA* strain, where the chromosomal copy of *lolA* was deleted and a complementing copy placed under arabinose control at the *araBAD* locus, MIC values were determined for a panel of antibiotics including **1**, **3a** and A22. The MIC analysis was performed at multiple arabinose concentrations (0% - 0.2%), allowing for different cellular levels of LolA to be examined. Upon depletion of LolA (0.00002% and 0% arabinose) a 32-fold sensitization to compounds **1**, **3a** and A22 was observed (Figure 5). In this experiment we also looked for interactions with known antibiotics of varying mechanism and chemical class and none of these demonstrated an enhancement close to this magnitude, apart from the cell wall-active compound fosfomycin which registered as much as a 16-fold sensitization. Several outer

membrane lipoproteins have been found to impact the structural integrity of the cell [8]. As such, mislocalization of lipoproteins, due to the absence of LolA, could well compromise the cell wall, resulting in the observed sensitization. Together these experiments provide further evidence of a profound chemical-genetic interaction between *lolA* and the thiourea containing compounds.

Using the conditional LolA depletion strain, we were also interested in investigating the effects of reduced *lolA* expression on cellular morphology. It has been well established that treatment with A22 results in a morphological transformation from rod-shaped cells to spherical [4] and as such, we wished to examine whether LolA depletion could elicit a similar phenotypic response. Phase contrast light microscopy images were taken from samples expressing (Figure 6B) or depleted of LolA (Figure 6C) and samples treated with A22 (Figure 6E) or **1** (Figure 6F). Indeed, depletion of LolA resulted in the change of the cell shape from rod to sphere, the same phenotypic transition shared by treatment with **1** or A22. Interestingly, this phenotype is also seen on depletion of MreB depletion [9].

Table 1 provides a detailed SAR study of compound **3a**, where the antibacterial activity of 22 structural analogs were studied using lab strains of *E. coli* (MG1655), *Bacillus subtilis* (168) and *Pseuomonas aeruginosa* (PA01). Similar to compound **1**, the thiourea-based compounds (series 3 in Table 1) were active against both Gram-negative species, but had no significant effect (MIC >256 μg/mL) when tested against the Gram-positive *B. subtilis*. Additionally, we looked at the effect that *lolA* overexpression had on each analog with a MIC <16 μg/mL in *E. coli* (data not shown). Each active structural analog was suppressed by LolA at high copy, indicative of a similar cellular mechanism. These results were consistent with the idea that compound **3a** and analogs work through the inhibition the lipoprotein chaperone LolA, as Gram-positive bacteria do not have the lipoprotein transport system due to the absence of an outer membrane. On the other hand, Gram-positive bacteria have been reported to have multiple homologs of MreB [10]. Two homologs, Mbl and MreBH, have been identified in *B.*

subtilis and their functional redundancy could account for the inactivity of the thiourea compounds within these species [11].

We explored the effects of substitutions on the benzyl group of the *S*-benzylisothiourea (series 3 in Table 1) as has been previously reported by Iwai *et al*. [12]. We observed similar trends, where most substitutions could be tolerated, only the presence of the strongly electron donating methoxy substituent (**3k**) completely abolished activity. However, potency was affected by the size and position of the substituent, with the moderately sized halogens, Cl and Br at position 4, being the most favourable (**3a** and **3f**); suggesting that an optimal size is required to fit within a proposed drug binding pocket. Dichloro subsititions were also very favourable, where the 2,4 dichloro substitution (**3e**) was the most potent compound in the series.

Retaining the 4-chlorobenzyl moiety, we explored some new chemical matter by turning our attention to the effects that increasing (**3m**, **3n**) or decreasing (**4d**) the chain length between the sulphur and the benzyl ring might have on activity. These modifications, as well as complete removal of the benzyl ring (not shown) rendered the compounds inactive, supporting the importance of this benzyl ring and its placement in relation to the sulphur atom. When the sulphur was replaced by nitrogen (**4a**), carbon (**4b**) or removed altogether (**4e**) activity is also lost. However, oxygen at this position retained activity (**4c**), suggesting some tolerance in modifications at this position. Further, an analog of A22 was created which replaced the hydrogen from both amines with methyl groups (**5a**). This modification completely abolished the antibacterial activity. Lastly, the addition of a methylene spacer between the sulphur and the amino groups (**4f**), also completely abolished the antibacterial activity. In summary, substitutions on the benzyl ring were the most tolerated, whereas other modifications largely resulted in a significant decrease in activity.

We previously characterized a physical interaction between **1** and LolA using saturation transfer double difference NMR (STDD NMR) [2c]. As such, we employed this technique to

investigate interactions between **3a** and **A22** with LolA *in vitro.* A sample of pure recombinant LolA (15 µM) was incubated with **3a** or A22 at concentrations ranging from 0-1000 µM. The resulting STDD NMR spectra revealed considerable intermolecular magnetization transfer from LolA to **3a** (Figure 7A), a process that is dependent upon a direct interaction between protein and ligand. This spectrum is depicted in comparison to the one-dimensional reference proton NMR spectrum of **3a** (Figure 7B). Correspondingly, no STD NMR spectrum could be obtained for compound **4b**, a structural analog with no antibacterial activity (data not shown). To further characterize the interaction, peak areas corresponding to the aromatic protons of **3a** and A22 were used to determine the normalized STD_{af} and plotted against compound concentration (Figure 7C and D). These data were fit to the best hyperbolic curve and as such the K_d for the interaction of LolA with **3a** was found to be 150 ± 50 µM (Figure 7C), while the K_d for the interaction with A22 was comparable at 200 ± 50 µM (Figure 7D). These K_d values are greater than that reported for compound **1** and LolA (~8 µM) [2c] or A22 and MreB (~1.3 µM) [6] but indicate nevertheless that these compounds show a *bona fide* interaction with LolA *in vitro*. It remains unclear why the binding affinity of the parent compound **1** to LolA is higher than that for **3a** or **A22**. One possible explanation is that the 3,4-dimethoxyphenethylamine portion of compound **1**, while not essential for antibacterial activity, could nonetheless be involved in additional interactions with LolA that increase its overall binding affinity.

In conclusion, we report here on the (acid-catalyzed) degradation of MAC13243 (**1**), a novel probe of lipoprotein targeting, into the active species *S-(*4-chlorobenzyl)isothiourea (**3a**). Accordingly, we chose to investigate whether **3a** and its structural analog A22 share a similar cellular mechanism to that reported for **1**. Our study demonstrated a strong high-copy suppression (16-fold MIC) of the action of both **3a** and A22, as demonstrated for compound 1 previously [2c]. To control for possible artifacts associated with overexpression, we also conducted LolA depletion experiments and demonstrated specific enhancement (32-fold sensitization) of the growth inhibition by **1**, **3a** and A22. Interestingly, **1**, **3a** and A22 all induce a

morphological transition from rod to round cells that is shared by depletion of the LolA protein. Finally, through STD NMR we characterized a physical interaction between LolA and both **3a** and A22, as we have seen for compound **1** previously [2c].

Notwithstanding the biochemical interactions recorded here for A22 and the thiourea compound **3a** with LolA**,** it remains a formal possibility that a yet uncharacterized interaction between MreB function in the bacterial cytoskeleton and the OM lipoprotein transport machinery is responsible for the observed chemical genetic interactions. The bacterial cell is increasingly recognized as a composition of a highly dense and interconnected genes and proteins, where we could envision inhibition of LolA or MreB having effects on the function of the other. MreB forms one of the most highly connected protein nodes within the cell [13], involved in critical cell processes such as chromosome segregation, cell wall synthesis and maintaining cellular morphology [14]. While the exact role of MreB remains enigmatic a large body of work implicates MreB in cell wall peptidoglycan synthesis [15]. Lipoproteins too are well known to interact with cell wall peptidoglycan in Gram-negative bacteria [16] and have recently been linked to the cell wall biosynthetic machinery [17]. Accordingly, a cell wall biosynthetic network that links MreB and LolA function could provide a composite target for A22 and related thiourea compounds.

Taken together, the results from this investigation are nevertheless most consistent with the conclusion that compound **1** and the thiourea compound series represented by **3a** and A22 act through a similar mechanism. Further we have characterized new chemical genetic and biochemical interactions with the LolA protein for the compound A22, thought to be a specific probe of the bacterial actin-like protein MreB. While strong biochemical and genetic evidence supports MreB as the target of this compound, and presumably also related compounds studied here [5a, 6, 18], the work presented here suggests that A22 and related thiourea compounds may inhibit the function of both MreB and LolA. Such a mechanism would put A22 in the company of several well-known antibiotics, including β-lactams, fluoroquinolones, D-cycloserine and fosfomycin, that are known to have multiple cellular targets [19].

Acknowledgements

We thank Hirotada Mori of the Nara Institute for providing the *lolA* expression clone used in these studies and Tomasz Czarny for assisting in the preparation of figures. This work was supported by an operating grant from the Canadian Institutes of Health Research (MOP-81330) and by a Canada Research Chair award to E.D.B.

References

1. Falconer, S. B.; Czarny, T. L.; Brown, E. D., Antibiotics as probes of biological complexity. *Nat Chem Biol* **2011,** *7* (7), 415-23.
2. (a) Burdine, L.; Kodadek, T., Target identification in chemical genetics: the (often) missing link. *Chem Biol* **2004,** *11* (5), 593-7; (b) Parsons, A. B.; Lopez, A.; Givoni, I. E.; Williams, D. E.; Gray, C. A.; Porter, J.; Chua, G.; Sopko, R.; Brost, R. L.; Ho, C. H.; Wang, J.; Ketela, T.; Brenner, C.; Brill, J. A.; Fernandez, G. E.; Lorenz, T. C.; Payne, G. S.; Ishihara, S.; Ohya, Y.; Andrews, B.; Hughes, T. R.; Frey, B. J.; Graham, T. R.; Andersen, R. J.; Boone, C., Exploring the mode-of-action of bioactive compounds by chemical-genetic profiling in yeast. *Cell* **2006,** *126* (3), 611-25; (c) Pathania, R.; Zlitni, S.; Barker, C.; Das, R.; Gerritsma, D. A.; Lebert, J.; Awuah, E.; Melacini, G.; Capretta, F. A.; Brown, E. D., Chemical genomics in Escherichia coli identifies an inhibitor of bacterial lipoprotein targeting. *Nat Chem Biol* **2009,** *5* (11), 849-56; (d) Giaever, G.; Shoemaker, D. D.; Jones, T. W.; Liang, H.; Winzeler, E. A.; Astromoff, A.; Davis, R. W., Genomic profiling of drug sensitivities via induced haploinsufficiency. *Nat Genet* **1999,** *21* (3), 278-83; (e) Li, X.; Zolli-Juran, M.; Cechetto, J. D.; Daigle, D. M.; Wright, G. D.; Brown, E. D., Multicopy suppressors for novel antibacterial compounds reveal targets and drug efflux susceptibility. *Chem Biol* **2004,** *11* (10), 1423-30.
3. Narita, S.; Matsuyama, S.; Tokuda, H., Lipoprotein trafficking in Escherichia coli. *Arch Microbiol* **2004,** *182* (1), 1-6.
4. Iwai, N.; Nagai, K.; Wachi, M., Novel S-benzylisothiourea compound that induces spherical cells in Escherichia coli probably by acting on a rod-shape-determining protein(s) other than penicillin-binding protein 2. *Biosci Biotechnol Biochem* **2002,** *66* (12), 2658-62.
5. (a) Gitai, Z.; Dye, N. A.; Reisenauer, A.; Wachi, M.; Shapiro, L., MreB actin-mediated segregation of a specific region of a bacterial chromosome. *Cell* **2005,** *120* (3), 329-41; (b) Kruse, T.; Blagoev, B.; Lobner-Olesen, A.; Wachi, M.; Sasaki, K.; Iwai, N.; Mann, M.; Gerdes, K., Actin homolog MreB and RNA polymerase interact and are both required for chromosome segregation in Escherichia coli. *Genes Dev* **2006,** *20* (1), 113-24.
6. Bean, G. J.; Flickinger, S. T.; Westler, W. M.; McCully, M. E.; Sept, D.; Weibel, D. B.; Amann, K. J., A22 disrupts the bacterial actin cytoskeleton by directly binding and inducing a low-affinity state in MreB. *Biochemistry* **2009,** *48* (22), 4852-7.
7. Donald, R. G.; Skwish, S.; Forsyth, R. A.; Anderson, J. W.; Zhong, T.; Burns, C.; Lee, S.; Meng, X.; LoCastro, L.; Jarantow, L. W.; Martin, J.; Lee, S. H.; Taylor, I.; Robbins, D.; Malone, C.; Wang, L.; Zamudio, C. S.; Youngman, P. J.; Phillips, J. W., A Staphylococcus aureus fitness test platform for mechanism-based profiling of antibacterial compounds. *Chem Biol* **2009,** *16* (8), 826-36.
8. (a) Mizushima, S., Post-translational modification and processing of outer membrane prolipoproteins in Escherichia coli. *Mol Cell Biochem* **1984,** *60* (1), 5-15; (b) Cascales, E.; Bernadac, A.; Gavioli, M.; Lazzaroni, J. C.; Lloubes, R., Pal lipoprotein of Escherichia coli plays a major role in outer membrane integrity. *J Bacteriol* **2002,** *184* (3), 754-9; (c) Ohara, M.; Wu, H.

C.; Sankaran, K.; Rick, P. D., Identification and characterization of a new lipoprotein, NlpI, in Escherichia coli K-12. *J Bacteriol* **1999,** *181* (14), 4318-25.
9. Wachi, M.; Doi, M.; Tamaki, S.; Park, W.; Nakajima-Iijima, S.; Matsuhashi, M., Mutant isolation and molecular cloning of mre genes, which determine cell shape, sensitivity to mecillinam, and amount of penicillin-binding proteins in Escherichia coli. *J Bacteriol* **1987,** *169* (11), 4935-40.
10. Schirner, K.; Errington, J., Influence of heterologous MreB proteins on cell morphology of Bacillus subtilis. *Microbiology* **2009,** *155* (Pt 11), 3611-21.
11. Kawai, Y.; Asai, K.; Errington, J., Partial functional redundancy of MreB isoforms, MreB, Mbl and MreBH, in cell morphogenesis of Bacillus subtilis. *Mol Microbiol* **2009,** *73* (4), 719-31.
12. Iwai, N.; Fujii, T.; Nagura, H.; Wachi, M.; Kitazume, T., Structure-activity relationship study of the bacterial actin-like protein MreB inhibitors: effects of substitution of benzyl group in S-benzylisothiourea. *Biosci Biotechnol Biochem* **2007,** *71* (1), 246-8.
13. Butland, G.; Peregrin-Alvarez, J. M.; Li, J.; Yang, W.; Yang, X.; Canadien, V.; Starostine, A.; Richards, D.; Beattie, B.; Krogan, N.; Davey, M.; Parkinson, J.; Greenblatt, J.; Emili, A., Interaction network containing conserved and essential protein complexes in Escherichia coli. *Nature* **2005,** *433* (7025), 531-7.
14. Cabeen, M. T.; Jacobs-Wagner, C., Bacterial cell shape. *Nat Rev Microbiol* **2005,** *3* (8), 601-10.
15. White, C. L.; Gober, J. W., MreB: pilot or passenger of cell wall synthesis? *Trends in microbiology* **2012,** *20* (2), 74-9.
16. Braun, V.; Wu, H. C., *Lipoproteins, structure, function, biosythesis and model for protein export*. Elsevier Science: Amsterdam, 1994; Vol. 27, p 319-344.
17. (a) Paradis-Bleau, C.; Markovski, M.; Uehara, T.; Lupoli, T. J.; Walker, S.; Kahne, D. E.; Bernhardt, T. G., Lipoprotein cofactors located in the outer membrane activate bacterial cell wall polymerases. *Cell* **2010,** *143* (7), 1110-20; (b) Typas, A.; Banzhaf, M.; van den Berg van Saparoea, B.; Verheul, J.; Biboy, J.; Nichols, R. J.; Zietek, M.; Beilharz, K.; Kannenberg, K.; von Rechenberg, M.; Breukink, E.; den Blaauwen, T.; Gross, C. A.; Vollmer, W., Regulation of peptidoglycan synthesis by outer-membrane proteins. *Cell* **2010,** *143* (7), 1097-109.
18. Kruse, T.; Moller-Jensen, J.; Lobner-Olesen, A.; Gerdes, K., Dysfunctional MreB inhibits chromosome segregation in Escherichia coli. *EMBO J* **2003,** *22* (19), 5283-92.
19. Hopkins, A. L., Network pharmacology: the next paradigm in drug discovery. *Nat Chem Biol* **2008,** *4* (11), 682-90.
20. Link, A. J.; Phillips, D.; Church, G. M., Methods for generating precise deletions and insertions in the genome of wild-type Escherichia coli: application to open reading frame characterization. *J Bacteriol* **1997,** *179* (20), 6228-37.
21. Datsenko, K. A.; Wanner, B. L., One-step inactivation of chromosomal genes in Escherichia coli K-12 using PCR products. *Proc Natl Acad Sci U S A* **2000,** *97* (12), 6640-5.
22. Campbell, T. L.; Brown, E. D., Characterization of the depletion of 2-C-methyl-D-erythritol-2,4-cyclodiphosphate synthase in Escherichia coli and Bacillus subtilis. *J Bacteriol* **2002,** *184* (20), 5609-18.
23. Dennis, J. J.; Zylstra, G. J., Plasposons: modular self-cloning minitransposon derivatives for rapid genetic analysis of gram-negative bacterial genomes. *Appl Environ Microbiol* **1998,** *64* (7), 2710-5.
24. Kitagawa, M.; Ara, T.; Arifuzzaman, M.; Ioka-Nakamichi, T.; Inamoto, E.; Toyonaga, H.; Mori, H., Complete set of ORF clones of Escherichia coli ASKA library (a complete set of E. coli K-12 ORF archive): unique resources for biological research. *DNA Res* **2005,** *12* (5), 291-9.

Table 1: Structure activity relationships of S-(4-chlorobenzyl)isothiourea derivatives[1]

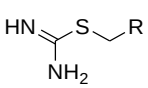

Compound Series **3**

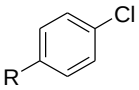

Compound Series **4**

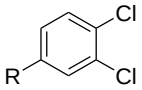

Compound Series **5**

Cmpd	*R*	Organism	MIC (µg/mL)
1	n/a	*E. coli* *B. subtilis* *P. aeruginosa*	8 256 32
2	n/a	*E. coli* *B. subtilis* *P. aeruginosa*	>256 nd nd
3a	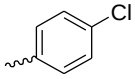	*E. coli* *B. subtilis* *P. aeruginosa*	2 >256 16
3b	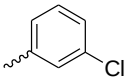	*E. coli* *B. subtilis* *P. aeruginosa*	64 >256 >256
3c	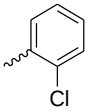	*E. coli* *B. subtilis* *P. aeruginosa*	16 >256 64
3d (A22)	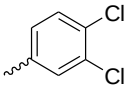	*E. coli* *B. subtilis* *P. aeruginosa*	2 >256 16
3e	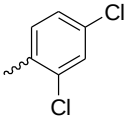	*E. coli* *B. subtilis* *P. aeruginosa*	1 >256 32
3f	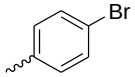	*E. coli* *B. subtilis* *P. aeruginosa*	4 >256 16
3g	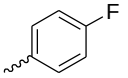	*E. coli* *B. subtilis* *P. aeruginosa*	16 >256 16
3h	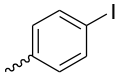	*E. coli* *B. subtilis* *P. aeruginosa*	16 >256 32
3i		*E. coli* *B. subtilis* *P. aeruginosa*	64 >256 32
3k	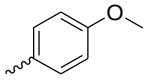	*E. coli* *B. subtilis* *P. aeruginosa*	>256 >256 32
3l	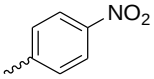	*E. coli* *B. subtilis* *P. aeruginosa*	32 >256 64
3m	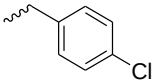	*E. coli* *B. subtilis* *P. aeruginosa*	>256 >256 128
3n	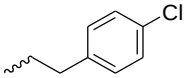	*E. coli* *B. subtilis* *P. aeruginosa*	>256 >256 128
4a	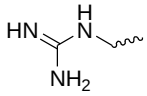	*E. coli* *B. subtilis* *P. aeruginosa*	256 >256 128
4b	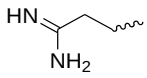	*E. coli* *B. subtilis* *P. aeruginosa*	>256 >256 128
4c	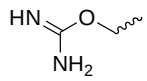	*E. coli* *B. subtilis* *P. aeruginosa*	32 >256 32
4d	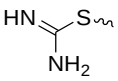	*E. coli* *B. subtilis* *P. aeruginosa*	>256 4 64
4e		*E. coli* *B. subtilis* *P. aeruginosa*	>256 >256 128
4f	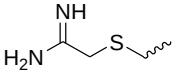	*E. coli* *B. subtilis* *P. aeruginosa*	>256 >256 128
5a	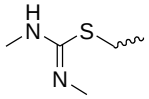	*E. coli* *B. subtilis* *P. aeruginosa*	256 >256 256

[1] Minimum inhibitory concentrations (MIC) were determined in liquid LB media. Overnight cultures were diluted 1:100 into fresh media and grown to an OD_{600} of 0.4 and then diluted 1:100000. Diluted cells (100 µL) were added to 96 well microplates containing serially diluted compound to a concentration of 1-256 µg/mL in a final volume of 200 µL and incubated at 37°C for 16 hours without shaking, except for *B. subtilis* which required aeration at 250 rpm. The lowest concentration at which the OD_{600} was below 0.05 was deemed MIC. Bacterial strains were *E. coli* MG1655*, B. subtilis* 168 *and P. aeruginosa* PAO1 (nd, not determined).

Table 2: Strains, plasmids and oligonucleotides used in this study

Strain	Description	Ref.
EB68	MG1655 (F^- λ^-)	[20]
EB2119	MG1655 (F^- λ^-) *araBAD*::*lolA*(optimal RBS)*kan*	This work
EB2120	MG1655 (F^- λ^-) *araBAD*::*lolA*(optimal RBS)*kan*Δ*lolA*	This work
Plasmid		
pKD46	Red recombinase expression plasmid for transformation of linear DNA in *E. coli*	[21]
pBS-*araBADkan*	pBluescript with Kan^R cassette inserted between *araBAD* flanking sequence	[22]
pBS-*araBADlolAkan*	pBluescript with *lolA* (optimal RBS) and Kan^R cassette inserted between *araBAD* flanking sequence	This work
p34S-CM	A source for a chloramphenicol resistance cassette	[23]
Oligonucleotide		
lolA-F[a]	5'-A**AGGAGG**AATAATGATGAAAAAAATT-3'	
lolA-R	5'-CTACTTACGTTGATCATCTAC-3'	
araC-F	5'-CGCCAGCAGCTCCGAATAGCGCCC-3'	
lolA-A	5'-GTCCATGGTGCTTTTGTTCGC-3'	
lolA-B	5'-TCGACCTGCAGGCATGCAAGCCATTATTCCTCAAATTACGTCACT-3'	
lolA-C	5'-GAGTGGCAGGGCGGGGCGTAACGTAAGTAGAGGCACCTGAGT-3'	
lolA-D	5'-CTCAGGGATTTCAACAGATAG-3'	
lolA-E	5'-TCTTCCATCGCCTGAGTTAG-3'	
lolA-F	5'-GGATATGCTCTACTCTGGGCC-3'	
CM-F	5'-AGTGACGTAATTTGAGGAATAATGGCTTGCATGCCTGCAGGTCGA-3'	
CM-R	5'-ACTCAGGTGCCTCTACTTACGTTACGCCCCGCCCTGCCACTC-3'	

[a] Bold face sequence indicates optimal ribosome binding site

Figure Legends

Figure 1. Breakdown Scheme of MAC13243. MAC13243 (**1**) is hydrolyzed at the triazine ring generating one molecule of 3,4-dimethoxyphenethylamine (**2**), one molecule of *S-(*4-chlorobenzyl)isothiourea (**3a**) and two molecules of formaldehyde. Also shown is the structure of A22 a close analog of **3a**.

Figure 2. Analysis and kinetics of compound degradation. To investigate the stability of compound **1**, samples of the compound at a final concentration of 250 µM were incubated in DMSO, H_20, 50 mM acetate buffer (pH 4) or 50 mM citrate buffer (pH 11) and examined using reverse phase HPLC. Chromatography was on a Symmetry C^{18} (4.6 x 150 mm; 3.5 µM) column from Waters (Mississauga, Ontario, Canada). Samples were eluted from the column with a 10 minute linear gradient from 95% buffer A (0.1% trifluoroacetic acid (TFA) in H_2O) to 97% Buffer B (0.1% TFA in acetonitrile). Analytes were visualized at 270 nm. A) HPLC trace for MAC13243 in DMSO at time zero (solid line), overlaid with the trace of MAC13243 incubated at pH 4 for 4 hours (dotted line). Peak identities were determined through mass spectrometry. LC-ESI-MS data were obtained by using an Agilent 1100 Series LC system (Agilent Technologies Canada, Inc.) and a QTRAP LC/MS/MS System (Applied Biosystems/MDS Sciex). B) Degradation profiles of **1** under each condition: (●) DMSO, (△) H_2O, (O) 50 mM acetate buffer (pH 4) and (▲) 50 mM citrate buffer (pH 11). Peak areas corresponding to **1** were plotted against time and fit to an exponential decay curve.

Figure 3. Compound 3a is the active breakdown component. The activity of compound **1** (●) and the major breakdown products, **2** (O) and **3a** (▼), were tested against *E. coli* MG1655. Cells were grown to an OD_{600} of 0.4 and subsequently diluted 1:100 000 into fresh Luria-Bertani

(LB) containing serially diluted compound. After 16 hours of incubation at 37°C the absorbance at 600 nm was recorded.

Figure 4. LolA at high copy suppresses the action of the thiourea compounds 3a and A22. *E. coli* strain AG1 harbouring plasmids pCA24N and pCA24N-LolA were from the ASKA collection [24]. Overnight cultures grown directly from frozen stocks in LB containing chloramphenicol (CM) were diluted 1:100 into 200 µL of fresh media and subsequently grown to an OD_{600} of 0.3. Cells were induced with 0.1 mM Isopropyl β-D-1-thiogalactopyranoside (IPTG) for 2 hours. Cultures were further diluted 1:500 and 2 µL of the diluted culture was spotted in duplicate on LB CM agar plates with or without 0.1 mM IPTG and containing 0, 2X, 4X, 8X and 16X the MIC of respective compounds. Plates were incubated at 37°C for 24 hours.

Figure 5. LolA depletion sensitizes *E. coli* to compound 1 and the thiourea compounds 3a and A22. The growth inhibitory effects compounds 1, 3a, A22 MAC13243, and a variety of antibiotics of diverse mechanism and chemical class were examined in a strain of *E. coli* (EB2120) where the expression of gene *lolA* is under the control of an arabinose-induced promoter. Primers *lolA*-F and *lolA*-R were used with Vent polymerase to PCR-amplify *lolA* from *E. coli* MG1655 chromosomal DNA. The PCR product, which placed a consensus ribosome binding site upstream of *lolA*, was cloned into the PmeI site of pBS-*araBADKan*. The resulting plasmid, pBS-*araBADlolAKan*, was cut with KpnI and SacI and the 2.6 kb fragment containing *lolA* was transformed into MG1655-pKD46. To screen for integration of *lolA* at the *araBAD* locus, chromosomal DNA was isolated from Kan^R colonies and used as a template in a PCR reaction with primers *araC*-F and *lolA*-R. A strain positive for *lolA* integration was termed EB2119. To create a conditionally complemented *lolA* deletion strain, EB2120, a double crossover PCR strategy was used to produce a linear fragment for transformation of EB2119. Primers *lolA*-A and *lolA*-B, *lolA*-C and *lolA*-D, and CM-F and CM-R were used with Vent

polymerase to amplify MG1655 chromosomal DNA or p34S-Cm DNA in the latter case. The PCR products were isolated and used as templates in a final reaction with primers *lolA*-A and *lolA*-D. The resulting product contained a chloramphenicol resistance cassette with its transcriptional promoter, but not its terminator, flanked by 500 bp homology to the regions upstream and downstream of *lolA*. The 1.4 kb product was transformed into EB2119, and replacement of native *lolA* was confirmed by PCR using primers *lolA*-E and CM-F and *lolA*-F and CM-R. Strain EB2120 was grown O/N at 37°C in the presence of 0.2% arabinose and subcultured to a final OD_{600} of 0.001 into LB media. Cells were grown to an OD_{600} of ~0.4-0.5 and 5 µL of culture was subsequently added to microwell plates containing serially diluted antibiotics ranging in concentration from 1-256 µg/mL in a final volume of 200 µL. MIC values were determined in the presence of (0.2%, 0.02%, 0.00002% and 0%) arabinose. Plates were incubated at 37°C for 18 hours. Fold sensitization was calculated based on MIC values determined under the LolA depletion condition in comparison to the fully complemented 0.2% arabinose condition. Depletion of LolA results in a 32-fold sensitization to MAC13243, TU-1 and A22.

Figure 6. LolA depletion and compound treatment leads to the formation of spherical cells. *E.coli* strains EB68 (wild type MG1655) and EB2120 (conditionally expresses gene lolA in response to arabinose; see legend to Figure 5) were grown overnight at 37°C in LB or LB media containing 0.2% arabinose. The cells were subcultured 1:100 into 5 mL LB media containing 0.1% D-fucose and grown until an OD_{600} ~ 0.5 was reached. The cells were washed once with fresh media. EB2120 was resuspended into LB containing 0.2% arabinose or 0.1% glucose. EB68 was resuspended in LB + A22 (10 µg/mL) or LB + compound **1** (10 µg/mL). Cells were then applied to poly-lysine treated microscope slides and examined by light microscopy at 1 hour intervals. Images were captured by a Q-colour 3 camera (Olympus, Mississauga, ON, Canada).

Figure 7. K_d determination using saturation transfer double difference (STDD) NMR. The interaction of compounds **3a** and A22 with LolA was examined using saturation transfer double difference NMR as described previously [2c]. A) STDD NMR spectrum of LolA/TU-1 interaction generated by selectively saturating the methyl region of LolA and obtaining the difference between the spectra of the ligand alone and the spectra of the ligand and protein complex. B) The 1D NMR reference spectrum for **3a**. The dissociation constants (K_d) for the interaction of **3a** with LolA interaction (C) and A22 with LolA (D) were obtained by plotting the calculated STD_{af} against increasing concentrations of compound. The 1D-STD titration was carried out by titrating 15 µM LolA with total ligand concentrations of 25, 50, 100, 200, 600 or 1000 µM.

Figure 1

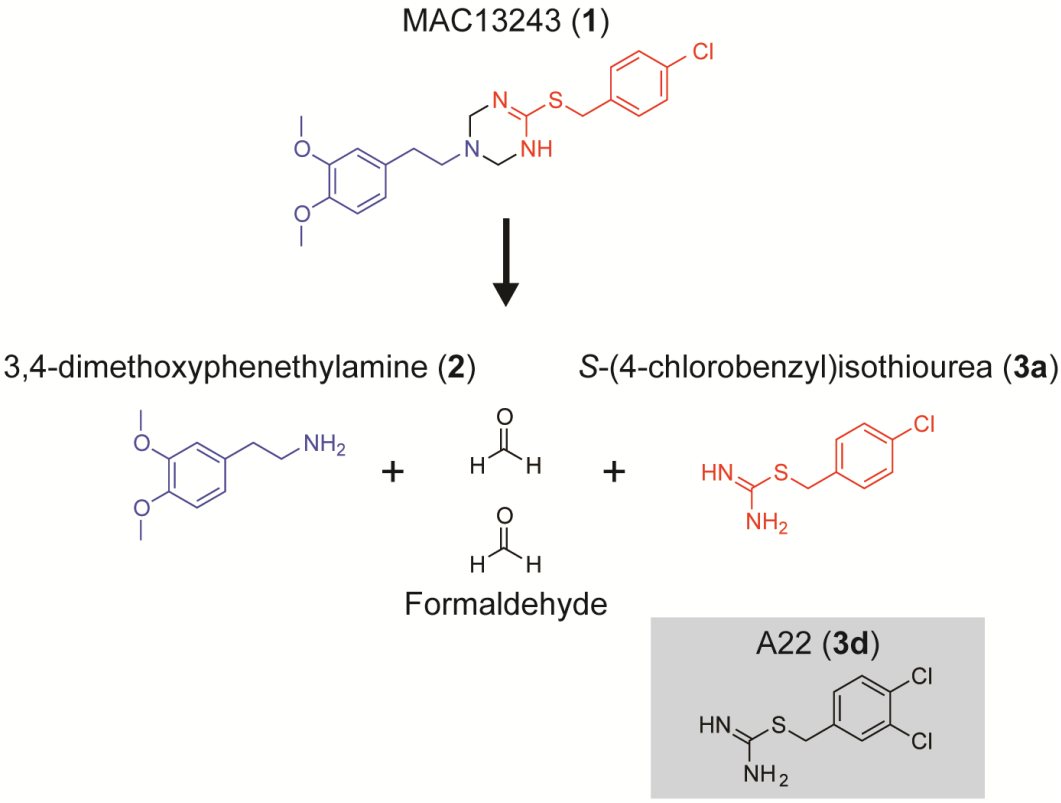
MAC13243 (1)
Cl
N
S
O
N
NH
O
3,4-dimethoxyphenethylamine (2)
S-(4-chlorobenzyl)isothiourea (3a)
NH2
+
O
H
H
O
H
H
+
HN
S
NH2
Cl
Formaldehyde
A22 (3d)
Cl
HN
S
NH2
Cl

Figure 2

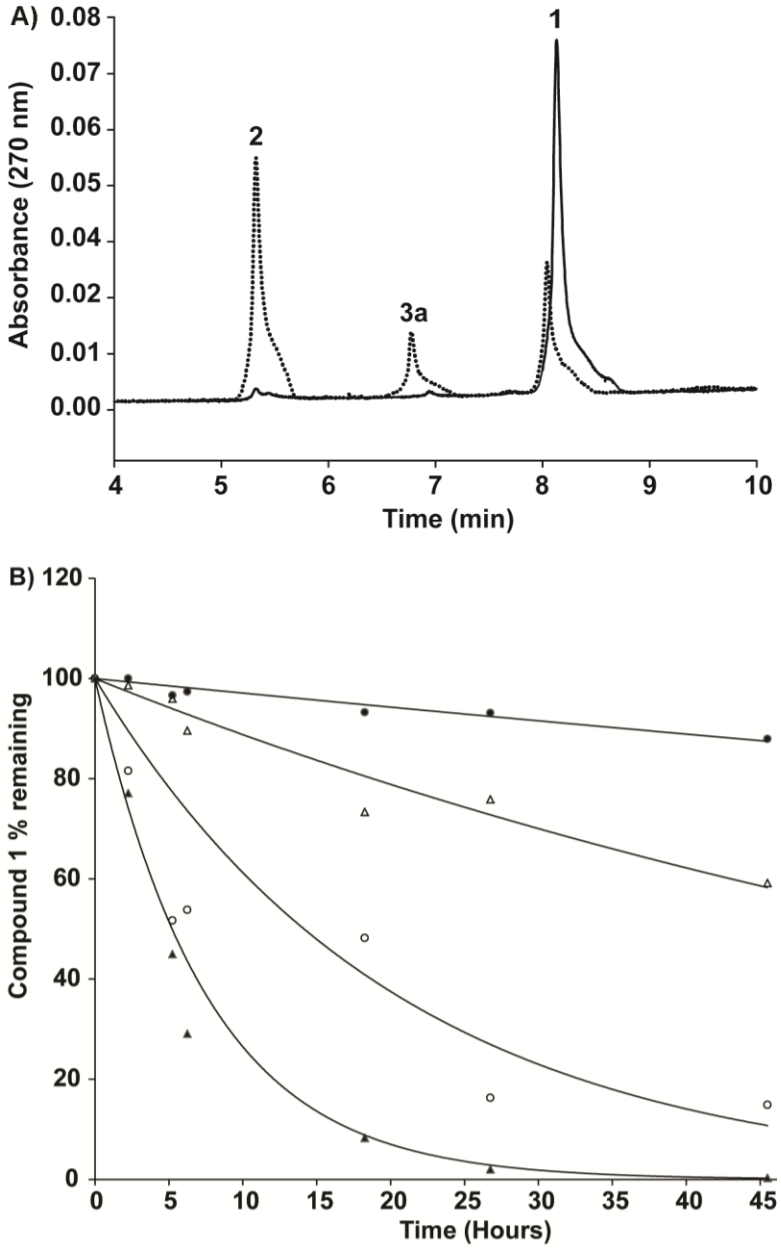
A)
Absorbance (270 nm)
0.08
0.07
0.06
0.05
0.04
0.02
0.01
0.00
1
2
3a
4
5
6
7
8
9
10
Time (min)
B)
Compound 1 % remaining
120
100
80
60
40
20
0
0
5
10
15
20
25
30
35
40
45
Time (Hours)

Figure 3

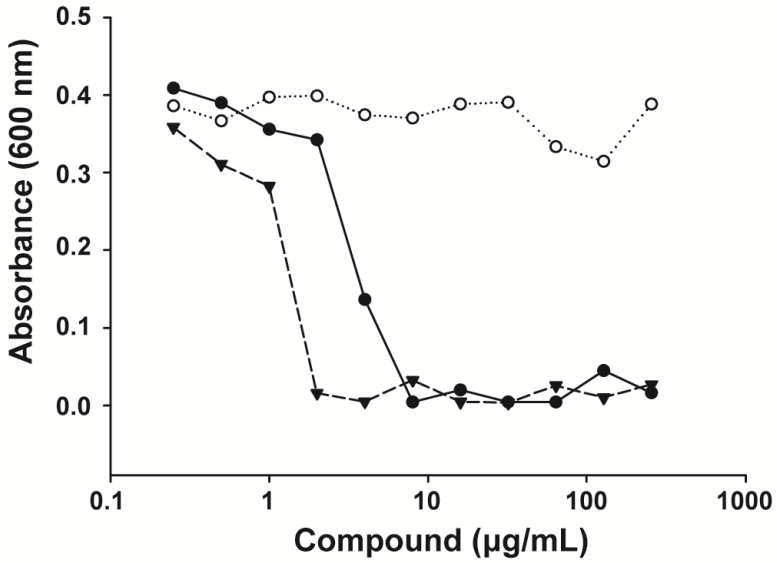
Absorbance (600 nm)
0.5
0.4
0.3
0.2
0.1
0.0
0.1
1
10
100
1000
Compound (µg/mL)

Figure 4

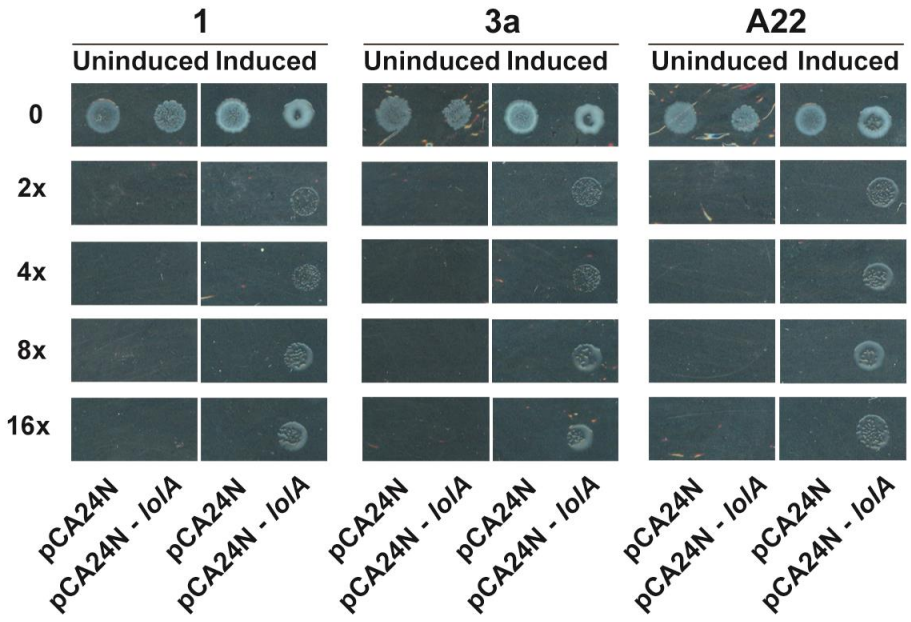
1
3a
A22
Uninduced Induced
Uninduced Induced
Uninduced Induced
0
2x
4x
8x
16x
pCA24N
pCA24N - lolA
pCA24N
pCA24N - lolA
pCA24N
pCA24N - lolA
pCA24N
pCA24N - lolA
pCA24N
pCA24N - lolA
pCA24N
pCA24N - lolA

Figure 5

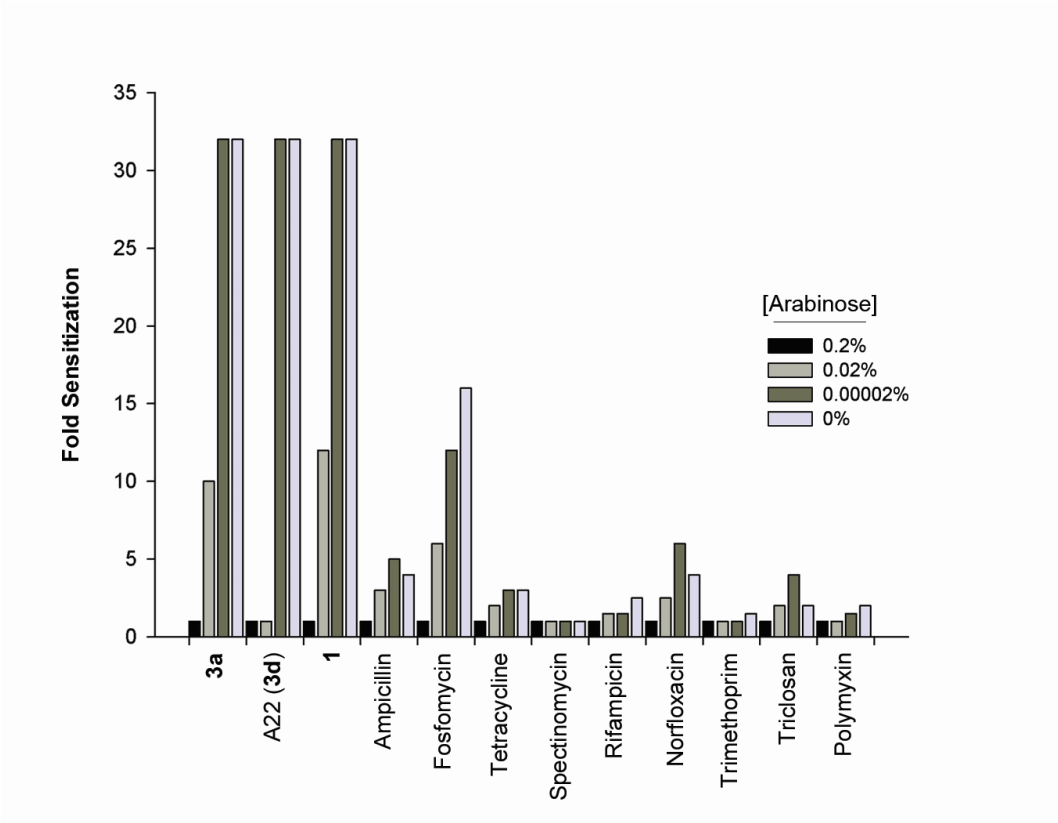
Fold Sensitization
35
30
25
20
15
10
5
0
[Arabinose]
0.2%
0.02%
0.00002%
0%
3a
A22 (3d)
1
Ampicillin
Fosfomycin
Tetracycline
Spectinomycin
Rifampicin
Norfloxacin
Trimethoprim
Triclosan
Polymyxin

Figure 6

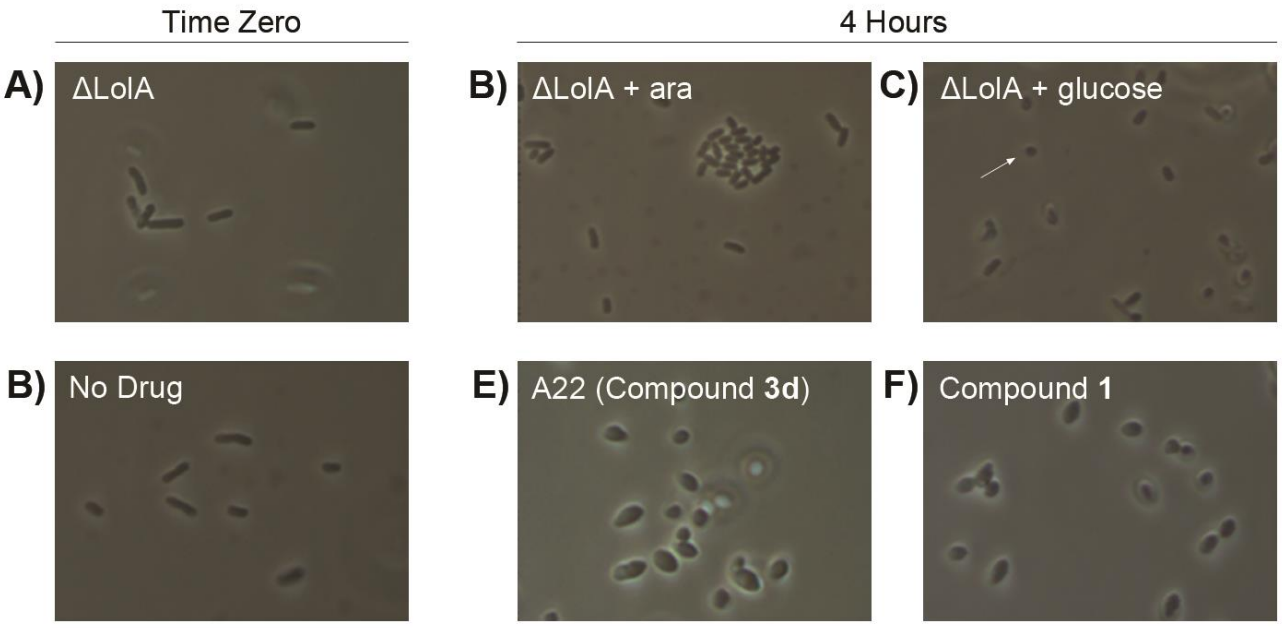
Time Zero
4 Hours
A)
ΔLolA
B)
ΔLolA + ara
C)
ΔLolA + glucose
B)
No Drug
E)
A22 (Compound 3d)
F)
Compound 1

Figure 7

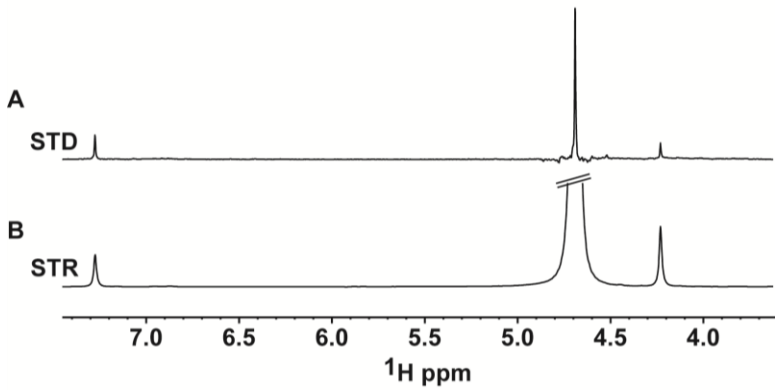
A
STD
B
STR
7.0
6.5
6.0
5.5
5.0
4.5
4.0
1H ppm

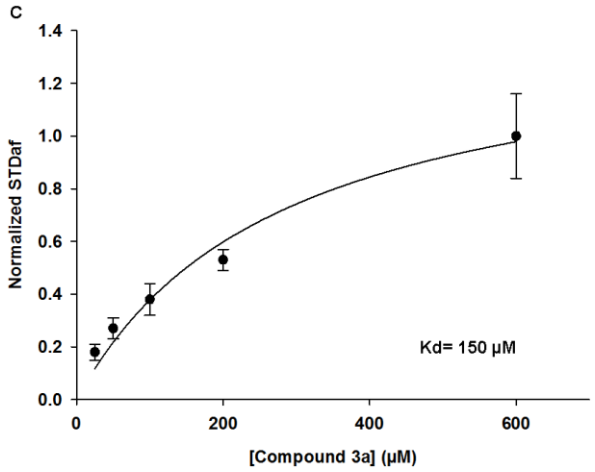
C
Normalized STDaf
1.4
1.2
1.0
0.8
0.6
0.4
0.2
0.0
0
200
400
600
[Compound 3a] (μM)
Kd= 150 μM

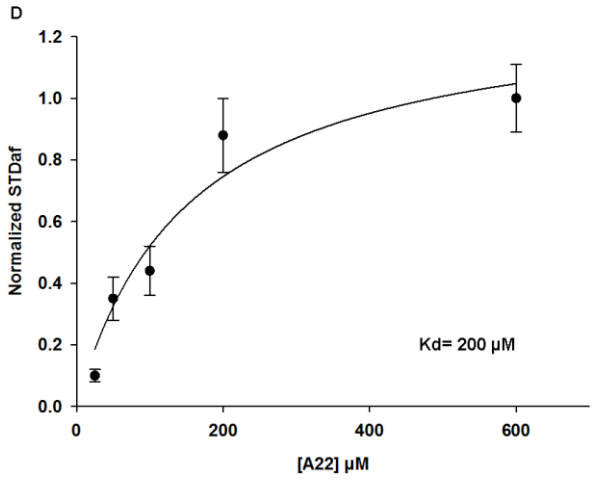
D
Normalized STDaf
1.2
1.0
0.8
0.6
0.4
0.2
0.0
0
200
400
600
[A22] μM
Kd= 200 μM